

Sampling the probability distribution of Type Ia Supernova lightcurve parameters in cosmological analysis

Mi Dai¹★ and Yun Wang^{1,2}★

¹Homer L. Dodge Department of Physics and Astronomy, University of Oklahoma, 440 W Brooks St., Norman, OK 73019, USA

²Infrared Processing and Analysis Center, California Institute of Technology, 770 South Wilson Avenue, Pasadena, CA 91125, USA

Accepted 2016 March 29. Received 2016 March 29; in original form 2015 May 19

ABSTRACT

In order to obtain robust cosmological constraints from Type Ia supernova (SN Ia) data, we have applied Markov Chain Monte Carlo (MCMC) to SN Ia lightcurve fitting. We develop a method for sampling the resultant probability density distributions (pdf) of the SN Ia lightcurve parameters in the MCMC likelihood analysis to constrain cosmological parameters, and validate it using simulated data sets. Applying this method to the ‘joint lightcurve analysis (JLA)’ data set of SNe Ia, we find that sampling the SN Ia lightcurve parameter pdf’s leads to cosmological parameters closer to that of a flat Universe with a cosmological constant, compared to the usual practice of using only the best-fitting values of the SN Ia lightcurve parameters. Our method will be useful in the use of SN Ia data for precision cosmology.

Key words: supernovae: general – cosmological parameters – cosmology: observations – dark energy.

1 INTRODUCTION

The use of Type Ia supernovae (SNe Ia) as calibrated standard candles has led to the discovery of dark energy – the accelerating expansion of the Universe (Riess et al. 1998; Perlmutter et al. 1999). The cause for the observed cosmic acceleration remains unknown. Probing the nature of cosmic acceleration is one of the most active areas of research today. For recent reviews, see Ratra & Vogeley (2008), Frieman, Turner & Huterer (2008), Caldwell & Kamionkowski (2009), Uzan (2010), Wang (2010), Li et al. (2011), Weinberg et al. (2013).

There are major ongoing and planned observational projects to illuminate the nature of cosmic acceleration. These include the ongoing Dark Energy Survey (DES) (Bernstein et al. 2012);¹ the dedicated dark energy space mission Euclid, scheduled for launch in 2020 (Laureijs et al. 2011);² and the Large Synoptic Survey Telescope (LSST; Abell et al. 2009),³ which is under construction, with first light planned for 2019. Dark Energy is one of the main science areas for the Wide-Field Infrared Survey Telescope (WFIRST), which could be launched as early as 2023 (Spergel et al. 2015).

We can expect a dramatic increase in the quantity and quality of SN Ia data in the next decade and beyond. For $z < 1$, thousands of SNe Ia are expected from DES, and hundreds of thousands of SNe Ia are expected from LSST. WFIRST will observe thousands of SNe

Ia at $z > 1$. In order to use the SN Ia data in precision cosmology, it is important that we develop robust analysis techniques that can be applied to the observed SN Ia lightcurves.

In this paper, we apply Markov Chain Monte Carlo (MCMC) to SN Ia lightcurve fitting. We develop a method for sampling the resultant probability density distributions (pdf) of the SN Ia lightcurve parameters in the MCMC likelihood analysis to constrain cosmological parameters. Both of these are new approaches in SN Ia cosmology. We present our methodology in Section 2, and results in Section 3. We conclude with a summary and discussion in Section 4.

2 METHODOLOGY

As the mechanism of SNe Ia explosion is still unclear, empirical models are used for fitting SN Ia lightcurves. The lightcurve of an SN Ia can be characterized by its shape and colour, which can be corrected to reduce the intrinsic dispersion in SN Ia peak magnitudes. The shape correction utilizes the correlation between SN Ia peak brightness and decline time (brighter SNe Ia decline more slowly in brightness) (Pskovskii 1977; Branch 1981; Phillips 1993, 1999). The colour correction models the variation of SN Ia colours and dust extinction.

Following Betoule et al. (2014), we use the SALT2 model [first proposed in Guy et al. (2007), and updated in Guy et al. (2010) and Betoule et al. (2014)] for SN Ia lightcurve fitting. SALT2 provides an average spectral sequence and colour dispersion from the training of a subset of SN Ia lightcurves. For SALT2, The four SN Ia lightcurve parameters are: date of maximum light in the rest-frame B band, the amplitude of the spectral sequence (which is described

* E-mail: mdai@ou.edu (MD); wang@ipac.caltech.edu (YW)

¹ <http://www.darkenergysurvey.org/>

² <http://www.euclid-ec.org/>

³ <http://www.lsst.org/>

conventionally by the peak magnitude in the rest-frame B band), lightcurve shape, and colour. The date of maximum light is a nuisance parameter, since the distance-indicator properties of a SN Ia only depend on its peak magnitude, lightcurve shape, and colour. The default fitting procedure is minimizing a χ^2 to find the best-fitting lightcurve parameters from a 4D grid of parameter values. This grid method has its limitations: it may result in a local minimum, and the error estimate is sensitive to the choice of the grid size and the spacing of the grid points.

In this paper, we use MCMC method to fit for lightcurve parameters, using the SALT2 model in Betoule et al. (2014). The MCMC method has the following advantages over a grid-based method:

- (i) The posterior is drawn randomly from the proposed distribution; the true probability distribution is recovered given enough number of realizations.
- (ii) The statistics can be calculated using multiple chains that have converged, leading to robust error estimates.
- (iii) The resultant probability density functions (pdf) are smooth and can be utilized in the subsequent cosmological analysis.

2.1 The SALT2 model

The SALT2 model (Guy et al. 2007; Guy et al. 2010) is an empirical lightcurve model that provides an average spectral sequence and its first order variation. The model flux is defined as:

$$\frac{dF}{d\lambda}(p, \lambda) = x_0 \times [M_0(p, \lambda) + x_1 M_1(p, \lambda) + \dots] \times \exp[c CL(\lambda)] \quad (1)$$

Where p is the phase from the maximum light in the rest frame, λ is the rest-frame wavelength, M_0 and M_1 are the average spectral sequence and its first order variation, CL is the colour law which is independent of phase. The lightcurve parameters x_0 , x_1 , and c are determined by lightcurve fitting. To find the best-fitting parameters, the default method finds the minimum χ^2 using a grid-based method. The χ^2 is expressed as:

$$\chi^2 = (F_{\text{model}} - F_{\text{obs}}) C_{\text{SN}}^{-1} (F_{\text{model}} - F_{\text{obs}}), \quad (2)$$

where F_{obs} is the observed flux after calibration, F_{model} is the model flux integrated over the observing filter $T(\lambda(1+z))$:

$$F_{\text{model}} = (1+z) \int \lambda \frac{dF}{d\lambda}(p, \lambda) T(\lambda(1+z)) d\lambda. \quad (3)$$

The covariance matrix C_{SN} consists of three parts: a diagonal term of the model error, a regular matrix (not diagonal) term of colour dispersions (K -correction errors), an error matrix (for SNLS) or a diagonal term of the observational flux errors (for SN samples other than SNLS):

$$C_{\text{SN}} = D_{\text{model}} + C_{\text{model}} + C_{\text{obs}}. \quad (4)$$

The model parts of the covariance matrix are dependent on the lightcurve parameters; they are varied to minimize the χ^2 for a given set of lightcurve parameters.

We will now discuss in detail the uncertainties in the model fluxes [D_{model} term in equation (4)]. The model fluxes are calculated using equation (1) and equation (3). The model uncertainties are calculated as

$$\sigma_{\text{model}} = (f_0/f_{\text{total}}) \times S \times (V_0 + x_1^2 V_1 + 2x_1 V_{01})^{1/2} \times F_{\text{model}}. \quad (5)$$

where S , V_0 , V_1 and V_{01} are provided as part of the SALT2 model, and are dependent on phase and wavelength. Basically, V_0 is the

variance in M_0 , V_1 is the variance in M_1 , V_{01} is the covariance between M_0 and M_1 . S is a scale factor. f_0 is the main component of the model flux, which is M_0 integrated over the observing filter; f_{total} is the total model flux including the M_1 component (not including the colour term). When $f_{\text{total}} \leq 0$, the model uncertainty is set to be 100 times that of the model flux. Note that in the SALT2 code, $(V_0 + x_1^2 * V_1 + 2 * x_1 * V_{01})$ is set to 0.0001 when it becomes less than zero.

2.2 MCMC lightcurve fitting

We use COSMOMC as a generic sampler to generate multiple chains using the Metropolis–Hastings algorithm. We assume convergence when $R - 1 < 0.01$ using the Gelman and Rubin ‘R-1’ statistic (Brooks & Gelman 1998). For a detailed discussion on COSMOMC, see Lewis & Bridle (2002).

To implement SALT2 lightcurve fitting using MCMC, we first need to understand how the SALT2 default grid-based method works. In particular, how the covariance matrix from equation (4) is handled, since the contribution from model uncertainties depends on the values of the lightcurve parameters (which are being fitted). There is an optional ‘update weights’ feature in the public SALT2 code, but it seems not to be used by either Conley et al. (2011) or Betoule et al. (2014); we are only able to reproduce their results without using this option (see Section 3). However, by not updating the weights for the covariance matrix in the SALT2 code, it does not mean keeping the covariance matrix fixed. It means deriving a converged covariance matrix by doing the following:

- (i) Initial fit with x_1 fixed to be 0, without including model uncertainty.
- (ii) Second fit with x_1 allowed to vary, without including model uncertainty.
- (iii) Iterations of fits with model uncertainty included, until the changes in all parameters are less than 0.1 times the errors in the parameters.

At the beginning of each iteration in step 3, the covariance matrix is recalculated using the parameters from the previous step or iteration. And the covariance matrix is kept fixed during this iteration of the fit. In MCMC we cannot do the fit by steps as in the grid-based method, so we calculate the covariance matrix using fiducial lightcurve parameter values and keep it unchanged during the MCMC lightcurve fitting. We assume that likelihood $\propto \exp(-\chi^2/2)$, with χ^2 defined in equation (2), and carry out the following steps:

- (i) Perform a grid-based fit to obtain a set of fiducial values of lightcurve parameters (which are the best-fitting values from this fit).
- (ii) The covariance matrix C_{SN} is calculated using the fiducial values of the model and lightcurve parameters.
- (iii) An MCMC likelihood analysis is performed to obtain the lightcurve parameters, while fixing the covariance matrix to be that calculated using the fiducial lightcurve parameters.

A compelling reason for us to fix the covariance matrix for MCMC lightcurve fitting to be that calculated at fiducial values of the lightcurve parameters is as follows. The model uncertainty from equation (5) is dependent on the lightcurve parameters (especially x_1 and time of maximum flux), so it is varied as the lightcurve parameters are varied. For example, if x_1 is a very large number, it is possible that f_{total} will become negative, which means that the model uncertainty is set to 100 times that of the model value, leading to

a very small χ^2 – a numerical artefact that can bias the lightcurve fitting. We have found that simply updating the covariance matrix as the lightcurve parameters vary during the MCMC steps can lead to unreasonable results for the lightcurve parameters, since the model errors can be much larger when the lightcurve parameters fall out of the reasonable ranges.

To assess the implications of our choice of fixing the covariance matrix for MCMC lightcurve fitting, we have compared the lightcurve parameter results using two different fiducial values – one set contains the best-fitting results from a grid-based fit, the other set the best-fitting results from a grid-based fit without model errors. The lightcurve parameters we get from MCMC using the two different covariance matrices are very similar to each other (with a mean difference $\sim 10^{-4}$ for all three parameters used in a cosmological fit, i.e. m_B , x_1 , and c), and lead to almost identical cosmological constraints. This is not surprising, since the cosmological constraints are not very sensitive to the lightcurve parameters, as long as no erroneous lightcurve parameter values are used. We conclude that it is reasonable to fix the covariance matrix at fiducial values of the lightcurve parameters in MCMC lightcurve fitting.

2.3 Cosmological analysis

Having derived SN Ia lightcurve parameters using MCMC, we can use them to derive cosmological constraints. We follow the definition for the model magnitude in Conley et al. (2011):

$$m_{\text{mod}} = 5 \log_{10} \mathcal{D}_L - \alpha x_1 + \beta c + \mathcal{M}, \quad (6)$$

where \mathcal{D}_L is a redefined luminosity distance that is independent of the Hubble constant, α , β and \mathcal{M} are nuisance parameters which describe the shape and colour corrections of the lightcurve, and the SN absolute magnitude in combination with the Hubble constant. In order to model the dependence of SN Ia intrinsic brightness on the host galaxy mass, \mathcal{M} is defined as a function of the host galaxy stellar mass M_{host} (in units of solar masses):

$$\mathcal{M} = \begin{cases} \mathcal{M}_1 & \text{for } \log_{10} M_{\text{host}} < 10 \\ \mathcal{M}_2 & \text{for } \log_{10} M_{\text{host}} > 10 \end{cases} \quad (7)$$

The χ^2 is then

$$\chi^2 = \Delta \mathbf{m}^T \cdot \mathbf{C}^{-1} \cdot \Delta \mathbf{m}, \quad (8)$$

where $\Delta \mathbf{m} = \mathbf{m}_B - \mathbf{m}_{\text{mod}}$, and m_B is calculated by $m_B = -2.5 \log_{10}(x_0) + 10.635$ (Mosher et al. 2014). \mathbf{C} is the covariance matrix. We use the same covariance matrix in our cosmological analysis as that used by Betoule et al. (2014). Note that m_{mod} is defined in equation (6).

In this paper we assume a flat Universe with constant dark energy equation of state w , since SN Ia data alone do not provide meaningful constraints on additional cosmological parameters. The Hubble constant free luminosity distance \mathcal{D}_L is defined as:

$$\mathcal{D}_L \equiv c^{-1} H_0 (1 + z_{\text{hel}}) r(z), \quad (9)$$

where z_{hel} is the heliocentric redshift, z is the CMB-frame redshift (i.e. the cosmological redshift), $r(z)$ is the comoving distance:

$$r(z) = c H_0^{-1} \Gamma(z) \quad (10)$$

$$\Gamma(z) = \int_0^z \frac{dz'}{E(z')} \quad (11)$$

$$E(z) = H(z)/H_0. \quad (12)$$

With the assumption of flat Universe and constant w ,

$$H(z) \equiv \frac{\dot{a}}{a} = H_0 \sqrt{\Omega_m (1+z)^3 + \Omega_{DE} (1+z)^{3(1+w)}} \quad (13)$$

and $\Omega_m + \Omega_{DE} = 1$ (the radiation contribution is negligible here).

2.4 Pdf sampling

The MCMC analysis gives the marginalized pdf's of the lightcurve parameters. Those pdf's contain the distribution and error information of the lightcurve parameters and can be used in a cosmological analysis. We have developed a method to sample the pdf's, and derive cosmological results by combining results from different sets of lightcurve parameters drawn from the pdf's, as described below.

For each SN, we choose N points with equal probability intervals from the pdf of each lightcurve parameter, x_0 , x_1 and c , with probabilities equal to P_1, P_2, \dots, P_N . This gives N^3 sets of lightcurve parameters, with each set having the same SNe with different values of lightcurve parameters. We then use these sets of lightcurve parameters to fit cosmology, resulting in N^3 sets of cosmological parameters. We combine the results in the following way to get the combined cosmological parameters:

$$\mathbf{s} = \frac{\sum_{i,j,k} P_i P_j P_k \mathbf{s}_{ijk}}{\sum_{i,j,k} P_i P_j P_k}, \quad (14)$$

where \mathbf{s} are the cosmological parameters from sampling the pdf's of the lightcurve parameters, \mathbf{s}_{ijk} are the cosmological parameters derived from the data set with a given set of lightcurve parameters drawn from the pdf's of the lightcurve parameters. The cosmological parameters from different data sets are weighted by the product of the relative probabilities of the three lightcurve parameters, P_i , P_j , and P_k . Using only lightcurve parameters that correspond to the peaks of the pdf's gives $P_i = P_j = P_k = 1$; this is similar to the usual practice of using only the best-fitting lightcurve parameters in the grid-based method for SALT2 (which is equivalent to using the peaks of the mean likelihood distributions from MCMC).

It is not practical to densely sample the pdf's of the lightcurve parameters. In order to gauge how the cosmological parameter constraints depend on the sampling density of the lightcurve parameter pdf's, we study the following cases:

(i) **N = 3.** We choose three points from the pdf, with the probabilities $P_1 = 1$ and $P_2 = P_3 = 1/2$. This results in 3 points on the pdf: the peak, and the half height point on either side of the peak.

(ii) **N = 7.** We choose seven points on the pdf, $P_1 = 1$ (the peak), $P_2 = P_3 = 1/2$, $P_4 = P_5 = 3/4$, and $P_6 = P_7 = 1/4$. This divides the pdf in 1/4 segments in height, resulting in three points on either side of the peak.

(iii) **N = 15.** In this case 15 points are chosen from the pdf, the probabilities are 1, 1/2, 3/4, 1/4, 7/8, 5/8, 3/8, 1/8.

(iv) **N = 19.** When dividing the pdf into 10 equal probability intervals with probabilities $P_i = i/10$ ($i = 1, 2, \dots, 10$), we get 19 points on each pdf.

We will show that pdf sampling is converged with increased N in Section 3.4.

3 RESULTS

We have applied our methodology for SN Ia lightcurve fitting using MCMC and constraining cosmology with sampling the pdf's of SN Ia lightcurve parameters to the 'joint lightcurve analysis (JLA)' data set of SNe Ia from Betoule et al. (2014), which combines the SNLS

and SDSS data of SNe Ia in a consistent, well-calibrated manner. We do our MCMC lightcurve fitting using the calibrated photometric data provided by Betoule et al. (2014). The JLA sample, as an extension to the C11 Compilation (Conley et al. 2011), contains a combination of data sets of 740 spectroscopically confirmed SNe Ia from several low- z samples ($z < 0.1$) (mostly Hamuy et al. 1996; Riess et al. 1999; Jha et al. 2006; Hicken et al. 2009; Contreras et al. 2010), the full three-year SDSS-II supernova survey ($0.05 < z < 0.4$) (Sako et al. 2014), the first three years data of the SNLS survey ($0.2 < z < 1$) (Guy et al. 2010; Conley et al. 2011) and a couple of high redshift HST SNe ($0.7 < z < 1.4$) (Riess et al. 2007). The photometry of SDSS and SNLS is recalibrated. The SALT2 model is retrained using the joint data set.

3.1 Definitions

We will show comparative results on cosmological constraints using different sets of lightcurve parameters we have obtained in different approaches. These are:

(i) SALT2: this is the published lightcurve parameter set from Betoule et al. (2014), we use it directly in the cosmological analysis as the base of comparison to other sets.

(ii) GRID-SALT2: we obtain this set of lightcurve parameters by running the published version of the SALT2 code,⁴ adding in the bias correction term to the peak magnitude and the uncertainties in redshift, lensing and intrinsic dispersion to the magnitude uncertainties. All the values of the terms above are the same as those used in the JLA set as described in Betoule et al. (2014). This is supposed to reproduce the results of SALT2. All other sets of lightcurve parameters described in the following are processed as described here.

(iii) GRID: we use our own grid-based code using the SALT2 model to calculate the χ^2 ; this is an important cross-check, to ensure that we understand all the nuances of the public SALT2 code and its output. We will use this as the grid method to compare with our MCMC analysis. We obtain this GRID set of lightcurve parameters by minimizing the χ^2 using exactly the same approach as the SALT2 code does (i.e. using the function minimization package called MINUIT⁵). We expect to get the same values for the lightcurve parameters within numerical errors.

(iv) MCMC-LIKE: The MCMC chains can be used to calculate mean likelihood distributions; its maximum corresponds to the least χ^2 value from the grid method. If the grid method ever falls into a local minimum, the maximum likelihood value of the MCMC chains would instead give the correct global minimum upon convergence.

(v) MCMC-MARGE: The MCMC chains can be used to obtain marginalized one-dimensional distributions of the fitted parameters; these give the standard error distribution information from an MCMC analysis. For this MCMC-MARGE set, we use the means of the marginalized pdf's as lightcurve parameters for fitting cosmology (with no pdf sampling). We will discuss the pdf sampling results in Section 3.4.

In an MCMC analysis, the differences of the marginalized and the mean likelihood distributions indicate non-Gaussianity, although it is possible to have a non-Gaussian distribution where both curves are the same (Lewis & Bridle 2002). In general, the marginalized pdf differs more from the mean likelihood for parameters that are less well constrained by the data. Mean likelihood shows how good a fit you could expect if you drew a random sample from the

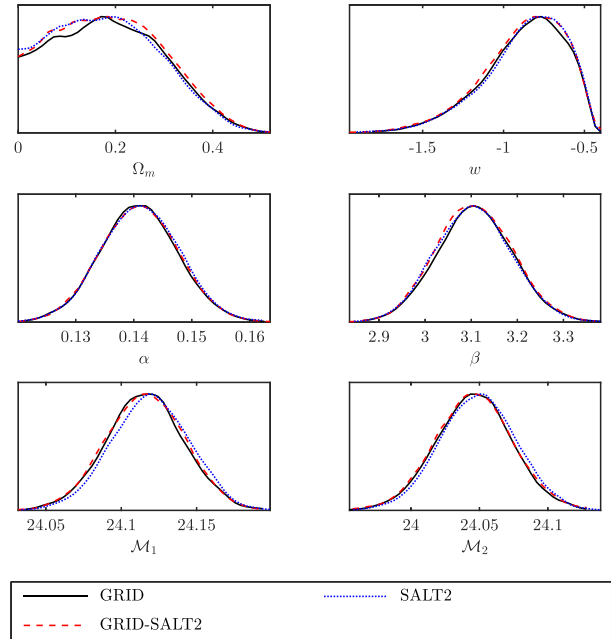


Figure 1. Mean likelihood pdf's of the parameters for the cosmological fit for the grid sets, using all 740 SNe from the JLA data set. Black solid lines represent the GRID set; red dashed lines represent the GRID-SALT2 set; blue dotted lines are for the SALT2 set.

marginalized distribution. It is customary to quote marginalized constraints in a cosmological analysis. We will follow this practice in this paper regarding the lightcurve parameters, except when we need to make a direct comparison with the grid-based method (which gives results that are equivalent to the mean likelihood). However, when showing the cosmological constraints, we give the mean likelihood pdf's instead, as our tests with simulated data sets show that the peaks of the mean likelihood pdf's of the cosmological parameters are less biased than the marginalized means. (For more details, see section 3.4.1.)

3.2 Reproducing the SALT2 results

We first compare results of the three grid sets – SALT2, GRID-SALT2 and GRID, to verify that our grid-based code is correct. In this cross-check exercise, we found that we are only able to reproduce the Betoule et al. (2014) results without using the “update weights” option in the public SALT2 code, but instead carrying out the steps as described in Section 2.2.

The lightcurve parameters from the three sets are very similar. Fig. 1 shows a comparison of the cosmological constraints from SALT2, GRID-SALT2, and GRID. As expected, all three approaches give nearly the same constraints on the cosmological and SN nuisance parameters.

3.3 MCMC versus GRID comparison

We now compare the results of MCMC and GRID. We find that the lightcurve parameters from the MCMC-LIKE set are also consistent with that from the GRID set. However, the lightcurve parameters of the MCMC-MARGE set are offset from the MCMC-LIKE (or the GRID) set for some SNe. The cosmological results are shown in Fig. 2. The MCMC-LIKE set gives similar cosmological constraint as the GRID set, as expected. The MCMC-MARGE set shows pdf's shifted from the MCMC-LIKE (or the GRID) set in Ω_m and w ; this

⁴ <http://supernovae.in2p3.fr/salt/doku.php>

⁵ <http://seal.web.cern.ch/seal/snapshot/work-packages/mathlibs/minuit>

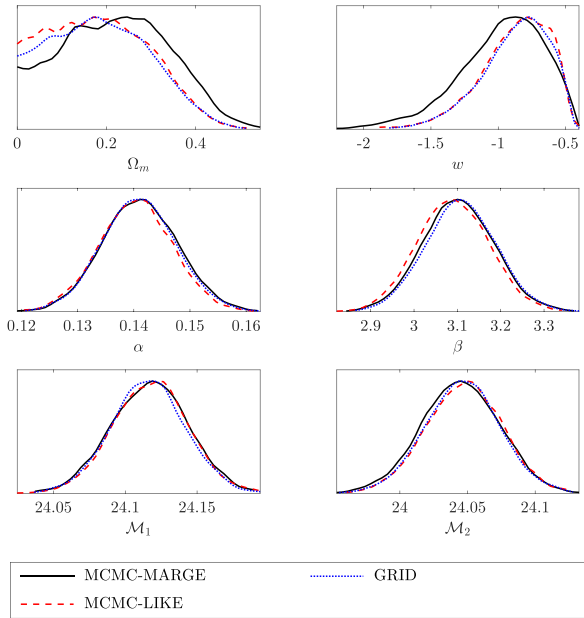


Figure 2. Mean likelihood pdf's of the parameters from the cosmological fit for the MCMC sets comparing with the GRID set, using all 740 SNe from the JLA data set. Black solid lines represent the MCMC-MARGE set; red dashed lines represent the MCMC-LIKE set; blue dotted lines represent the GRID set.

is not surprising given the difference between the marginalized and the mean likelihood in an MCMC analysis (see the discussion near the beginning of Section 3). The nuisance parameters are well constrained and have similar constraints in all sets.

The peaks of the mean likelihood pdf's and their 68 per cent confident intervals of the parameters are listed in Table 1. We find the approximate 68 per cent confidence levels by finding the parameter values where the probability has dropped by a factor of $e^{-1/2}$. Note that for some sets there is only one upper limit in Ω_m , because the pdf's are truncated at $\Omega_m = 0$ before the probability has dropped by a factor of $e^{-1/2}$. The grid methods (SALT2, GRID-SALT2, GRID) show similar values and errors. The MCMC-LIKE has consistent values with the grid methods but has slightly higher errors in Ω_m and w . The MCMC-MARGE set show even higher errors in w , but Ω_m and w are closer to the 'concordance model' of $\Omega_m = 0.27$ and $w = -1$.

3.4 Cosmological constraints from sampling the pdf's of SN Ia lightcurve parameters

We now present cosmological constraints derived from sampling the pdf's of SN Ia lightcurve parameters. For this work, we have to limit our analysis to SNe Ia with well-behaved lightcurve parameter

Table 1. Parameters from the cosmology fit using all 740 JLA SNe.

	Ω_m	w	α	β	\mathcal{M}_1	\mathcal{M}_2
SALT2	$0.196^{+0.116}$	$-0.795^{+0.261}_{-0.236}$	$0.141^{+0.008}_{-0.007}$	$3.107^{+0.078}_{-0.088}$	$24.118^{+0.027}_{-0.024}$	$24.050^{+0.026}_{-0.029}$
GRID-SALT2	$0.185^{+0.139}$	$-0.806^{+0.268}_{-0.267}$	$0.141^{+0.006}_{-0.007}$	$3.109^{+0.086}_{-0.090}$	$24.118^{+0.026}_{-0.029}$	$24.045^{+0.029}_{-0.028}$
GRID	$0.171^{+0.145}$	$-0.769^{+0.229}_{-0.282}$	$0.141^{+0.006}_{-0.007}$	$3.105^{+0.085}_{-0.076}$	$24.117^{+0.024}_{-0.027}$	$24.044^{+0.030}_{-0.025}$
MCMC-LIKE	$0.171^{+0.157}$	$-0.788^{+0.257}_{-0.282}$	$0.141^{+0.006}_{-0.007}$	$3.088^{+0.087}_{-0.082}$	$24.123^{+0.021}_{-0.032}$	$24.050^{+0.027}_{-0.030}$
MCMC-MARGE [†]	$0.246^{+0.125}_{-0.181}$	$-0.871^{+0.293}_{-0.338}$	$0.141^{+0.007}_{-0.007}$	$3.100^{+0.086}_{-0.083}$	$24.119^{+0.025}_{-0.029}$	$24.045^{+0.029}_{-0.030}$

[†]The MCMC-MARGE set uses the marginalized means of the lightcurve parameter pdf's.

Table 2. Problematic SNe.

	SN name
1	Lancaster
2	Patuxent
3	SDSS11206
4	SDSS14318
5	SDSS16619
6	SDSS16737
7	SDSS16793
8	SDSS19067
9	SDSS21510
10	SDSS21669
11	Torngasek

pdf's. For most SNe, the pdf's of their lightcurve parameters are well-behaved, single-peaked smooth bell curves. However, there are several exceptions with multi-peaked pdf profiles for the lightcurve parameters. We have tracked the multi-peaked profiles to data quality issues: some SNe have no data after the maximum light, some SNe have lightcurves with too few data points, or very noisy data. We exclude those problematic, multi-peaked SNe from our cosmological analysis. We also exclude other SNe that don't have any data in any bandpass after the peak magnitude as a quality cut. This results in a set of 729 SNe Ia; we will use only this set in our analysis from this point on.

The effects of excluding the 11 problematic SNe (listed in Table 2) from the cosmological analysis are shown in Fig. 3. The constraints on Ω_m and w are noticeably shifted by excluding these 11 SNe, indicating that cosmological results could be biased by including poor quality data. We observe the same effect both using the original JLA data and using our MCMC-fitted lightcurve parameters.

3.4.1 Tests with simulations

Before showing the results of pdf sampling applied to the JLA data set, we first show results from the simulated data sets to illustrate that pdf sampling gives less biased cosmological results than the usual practice without pdf sampling. To generate the simulated data sets, we replace the bias-corrected B -band peak magnitude (m_B) in the JLA data set with true peak magnitude calculated from a fiducial cosmological model, added with x_1^{random} and c^{random} randomly drawn from the lightcurve parameter pdf's we obtain using our MCMC lightcurve fitter, and a Gaussian scatter ($\mu = 0$, $\sigma^2 = 0.1^2$):

$$m_B = \mu(\Omega_m, w) - \alpha \times x_1^{\text{random}} + \beta \times c^{\text{random}} + \mathcal{M} + \mathcal{N}(0, 0.1^2) \quad (15)$$

The nuisance parameters α , β and \mathcal{M} are defined in equation (6), and are fixed with fiducial values.

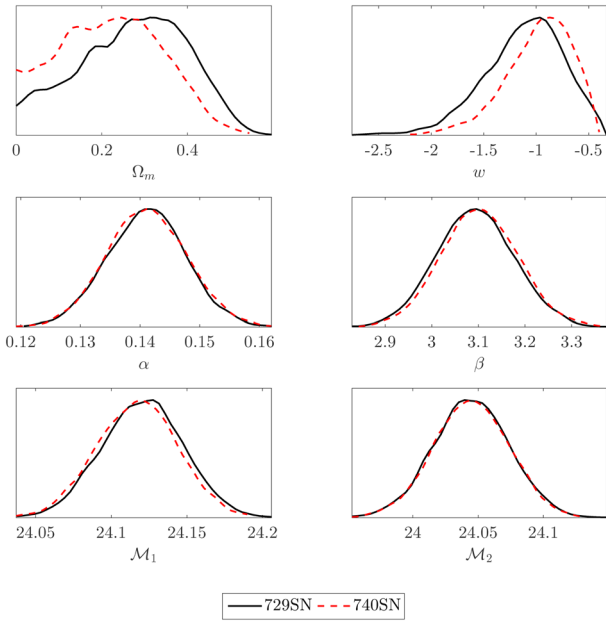


Figure 3. Mean likelihood pdf's of the parameters from the cosmological fit for different numbers of SNe Ia using the MCMC-MARGE set. Black solid lines show the results from 729 SNe excluding the 11 problematic SNe; red dashed lines represent the whole SNe sample including all 740 SNe from the JLA data set.

We generate 1000 sets of simulated data and perform cosmological analysis to each set of data, with and without pdf sampling. When applying pdf sampling to the simulated data set, we only sample the x_1 and c parameter, and only 3 points are chosen from each pdf to speed up the process. We list the input parameters and the means and standard deviations of the 1000 sets of resultant cosmological parameters in Table 3. We have shown both the peak values of the mean likelihood pdf and the means of the marginalized pdf. The two values and their standard deviations show differences in the Ω_m and w parameter, which is due to the differences in the meaning of the two kind of pdf's. We have briefly discussed the differences between the mean likelihood pdf and the marginalized pdf in Section 3.1. For more detailed discussions, see Lewis & Bridle (2002). Since the peaks of the mean likelihood pdf are less biased in general, we only show the mean likelihood pdf's for cosmological constraints in this paper. When quoting the peak values of the mean likelihood pdf's, comparing to not using pdf sampling, applying pdf sampling gives Ω_m and w that are closer to the input parameters, which is expected as pdf sampling utilizes more information from the lightcurve parameter pdf's. However, the standard deviations are larger in these two parameters when applying pdf sampling, as the values spread in larger ranges.

Table 3. Test with simulated data.

	Ω_m	w	α	β	\mathcal{M}_1	\mathcal{M}_2
input values	0.3	-1.0	0.14	3.1	24.11	24.04
w/o pdf (like ¹)	0.205 ± 0.098	-0.928 ± 0.196	0.152 ± 0.006	3.543 ± 0.088	24.114 ± 0.019	24.034 ± 0.021
w/ pdf (like ¹)	0.258 ± 0.111	-0.990 ± 0.288	0.152 ± 0.007	3.541 ± 0.089	24.123 ± 0.032	24.038 ± 0.036
w/o pdf (marge ²)	0.247 ± 0.057	-1.038 ± 0.163	0.152 ± 0.006	3.548 ± 0.088	24.112 ± 0.018	24.032 ± 0.020
w/ pdf (marge ²)	0.287 ± 0.055	-1.121 ± 0.181	0.148 ± 0.006	3.545 ± 0.089	24.111 ± 0.018	24.029 ± 0.020

Notes:¹The means and standard deviations of cosmological parameters of the 1000 simulated data sets, by quoting the peak values of the mean likelihood pdf's of the cosmological parameters;

²The means and standard deviations of cosmological parameters of the 1000 simulated data sets, by quoting the means of the marginalized pdf's of the cosmological parameters.

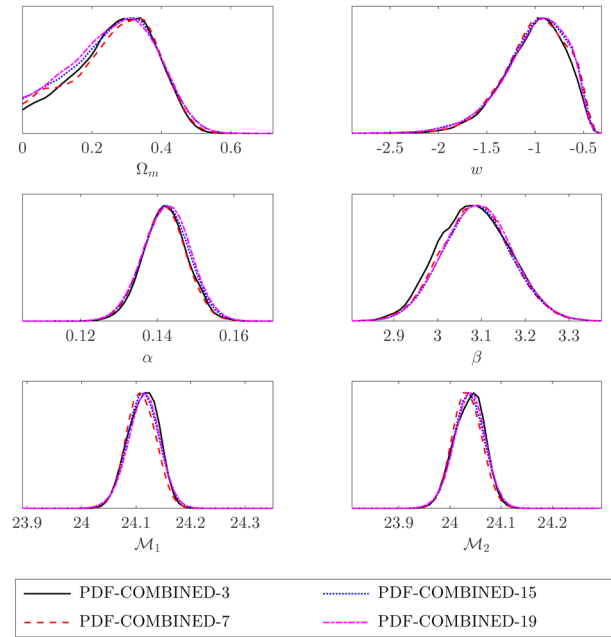


Figure 4. Mean likelihood pdf's of the parameters from the cosmological fit with sampling of the SN Ia lightcurve parameter pdf's, using 729 SNe Ia from the JLA data set (excluding 11 problematic ones). Black solid lines are results from sampling 3 points on each pdf (PDF-COMBINED-3); red dashed lines are results from sampling 7 points on each pdf (PDF-COMBINED-7); blue dotted lines are results from sampling 15 points on each pdf (PDF-COMBINED-15); magenta dash-dotted lines are results from sampling 19 points on each pdf (PDF-COMBINED-19).

3.4.2 Pdf sampling with the JLA data set

We now proceed to implement pdf sampling of the lightcurve parameters in our cosmological analysis, as described in Section 2.4, to the set of 729 SNe Ia, as described below:

(i) PDF-COMBINED-3: We draw $3^3 = 27$ sets of lightcurve parameters from the pdf's as described in Section 2.4. We also apply the same bias correction as used in the JLA set to each individual set of lightcurve parameters. The cosmological results of the individual sets are combined as described in Section 2.4 to obtain the cosmological results with pdf sampling of lightcurve parameters.

(ii) PDF-COMBINED-7: Similarly, $7^3 = 343$ sets of lightcurve parameters are drawn from the pdf's and the cosmological results are combined.

(iii) PDF-COMBINED-15 and PDF-COMBINED-19: $15^3 = 3375$ and $19^3 = 6859$ sets of lightcurve parameters are drawn

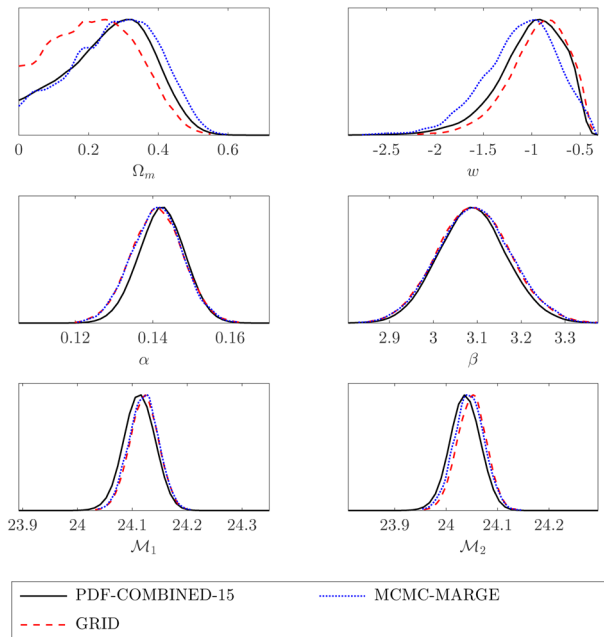


Figure 5. Mean likelihood pdf's of the parameters from the cosmological fit with and without sampling of the SN Ia lightcurve parameter pdf's, using 729 SNe Ia from the JLA data set (excluding 11 problematic ones). Black solid lines are results from sampling 15 points on each pdf (PDF-COMBINED-15); red dashed lines are results from using the GRID set; blue dotted lines are results from using the MCMC-MARGE set, without pdf sampling.

respectively. These ensure that the combined results have converged with increasing N (see Fig. 4).

We compare the results from using pdf sampling of lightcurve parameters with the GRID set and MCMC-MARGE (no lightcurve parameter pdf sampling), shown in Fig. 5. Since we have already shown that the pdf sampling results are converged with increasing N , we only show one set of results from using pdf sampling – PDF-COMBINED-15.

Note that the pdf's for Ω_m and w are shifted, compared to the results using the GRID set (grid-based method with no pdf sampling). When comparing with the results using only the marginalized mean values of the lightcurve parameters (without pdf sampling), the pdf's are also shifted, and pdf-sampling gives a little tighter constraints. The peak of the mean likelihood pdf's and their 68 per cent confidence intervals of the cosmological analysis using 729 SNe exclud-

ing the problematic ones are shown in Table 4. When excluding the problematic SNe, we get slightly larger Ω_m values, and the w values are closer to -1 . In Fig. 6, we show the corresponding 2D mean likelihood contours of the fitted parameters of PDF-COMBINED-15, GRID and MCMC-MARGE. It is interesting to note that pdf sampling of SN Ia lightcurve parameters, and using the means of the lightcurve parameter pdf's, leads to cosmological constraints closer to a flat Universe with a cosmological constant.

4 SUMMARY AND DISCUSSION

We have developed a method to utilize the pdf of SN Ia lightcurve parameters in cosmological analysis using SNe Ia. First, we have applied MCMC to SN Ia lightcurve fitting, in order to obtain smooth and well-behaved pdf's of SN Ia lightcurve parameters. Then we derived cosmological constraints with sampling of the pdf's of the SN Ia lightcurve parameters. For a complementary approach of sampling the underlying SN Ia population in cosmological model fitting, see March et al. (2011).

In order to validate our method, we applied it to 1000 sets of simulated SN Ia data. We found that compared to not using pdf sampling, applying pdf sampling gives Ω_m and w that are closer to the input parameters, which is expected as pdf sampling utilizes more information from the lightcurve parameter pdf's. We also found that the peak values of the mean likelihood pdf's are closer to the input values than the marginalized means.

Our method differs from the usual approach in two ways. (1) We use MCMC, instead of a grid-based method, in fitting the SN Ia lightcurve parameters; (2) We sampled the pdf's of the SN Ia lightcurve parameters in the cosmological analysis, instead of just using the peaks of the pdf's.

We have applied our method to the JLA data set of SNe Ia derived by Betoule et al. (2014), which combines the SNe Ia from SDSS and SNLS in a consistent, well-calibrated manner. Interestingly, we find that the resultant cosmological constraints are closer to that of a flat Universe with a cosmological constant, compared to the usual practice of using only the best-fitting values of the SN Ia lightcurve parameters.

The JLA set has a bias correction term which is determined using simulations generated by the *SNANA* software (Kessler et al. 2009), by comparing the reconstructed distance using SALT2-fitted lightcurve parameters to the simulation inputs (Betoule et al. 2014). We use this bias correction in our analysis, assuming that it is independent of the fitting technique. Ideally we should perform our own bias calculation by fitting the simulations with our MCMC lightcurve

Table 4. Parameters from the cosmology fit using 729 JLA SNe (excluding 11 problematic ones).

	Ω_m	w	α	β	\mathcal{M}_1	\mathcal{M}_2
SALT2	$0.238^{+0.115}_{-0.180}$	$-0.848^{+0.283}_{-0.270}$	$0.140^{+0.007}_{-0.006}$	$3.092^{+0.082}_{-0.092}$	$24.123^{+0.029}_{-0.024}$	$24.054^{+0.028}_{-0.030}$
GRID-SALT2	$0.258^{+0.104}_{-0.228}$	$-0.866^{+0.320}_{-0.306}$	$0.141^{+0.007}_{-0.006}$	$3.090^{+0.087}_{-0.083}$	$24.123^{+0.026}_{-0.028}$	$24.051^{+0.027}_{-0.030}$
GRID	$0.249^{+0.119}_{-0.336}$	$-0.830^{+0.291}_{-0.336}$	$0.141^{+0.007}_{-0.006}$	$3.093^{+0.083}_{-0.087}$	$24.124^{+0.024}_{-0.028}$	$24.053^{+0.026}_{-0.031}$
MCMC-LIKE	$0.263^{+0.120}_{-0.205}$	$-0.859^{+0.317}_{-0.359}$	$0.141^{+0.007}_{-0.007}$	$3.071^{+0.083}_{-0.080}$	$24.126^{+0.025}_{-0.030}$	$24.049^{+0.028}_{-0.031}$
MCMC-MARGE [†]	$0.312^{+0.118}_{-0.158}$	$-0.965^{+0.266}_{-0.420}$	$0.142^{+0.006}_{-0.007}$	$3.096^{+0.080}_{-0.087}$	$24.128^{+0.021}_{-0.033}$	$24.040^{+0.035}_{-0.024}$
PDF-COMBINED-3	$0.339^{+0.065}_{-0.161}$	$-0.910^{+0.288}_{-0.339}$	$0.142^{+0.006}_{-0.005}$	$3.076^{+0.092}_{-0.085}$	$24.124^{+0.023}_{-0.042}$	$24.046^{+0.025}_{-0.039}$
PDF-COMBINED-7	$0.335^{+0.072}_{-0.145}$	$-0.975^{+0.417}_{-0.288}$	$0.142^{+0.005}_{-0.006}$	$3.098^{+0.066}_{-0.093}$	$24.107^{+0.031}_{-0.026}$	$24.026^{+0.037}_{-0.023}$
PDF-COMBINED-15	$0.325^{+0.081}_{-0.162}$	$-0.916^{+0.351}_{-0.344}$	$0.143^{+0.005}_{-0.007}$	$3.084^{+0.079}_{-0.072}$	$24.116^{+0.026}_{-0.032}$	$24.036^{+0.031}_{-0.028}$
PDF-COMBINED-19	$0.309^{+0.098}_{-0.162}$	$-0.912^{+0.343}_{-0.330}$	$0.143^{+0.006}_{-0.006}$	$3.096^{+0.075}_{-0.086}$	$24.116^{+0.028}_{-0.029}$	$24.035^{+0.034}_{-0.026}$

[†]The MCMC-MARGE set uses the marginalized means of the lightcurve parameter pdf's.

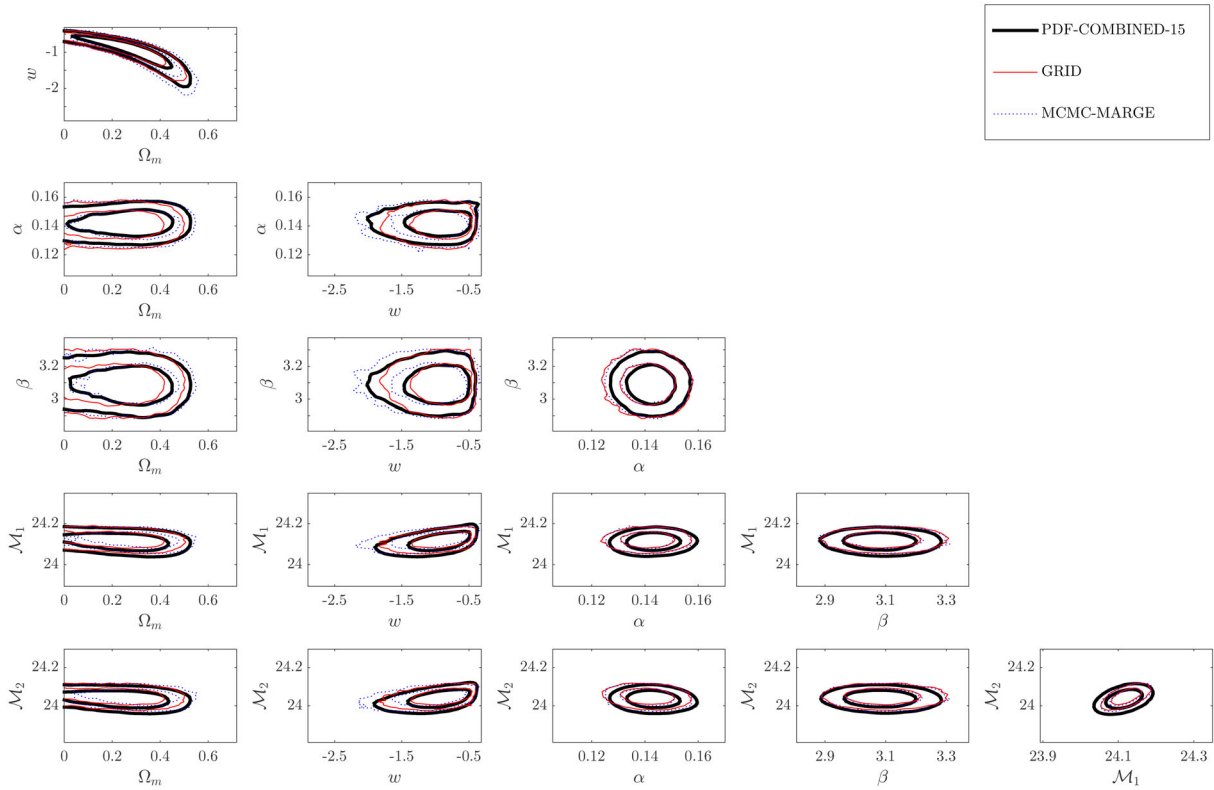


Figure 6. Joint confidence level contour plots from the cosmological fit with and without sampling of the SN Ia lightcurve parameter pdf's, using 729 SNe Ia from the JLA data set (excluding 11 problematic ones). The contours are 68 per cent and 95 per cent confidence levels. Thick black solid contours are results from sampling 15 points on each pdf (PDF-COMBINED-15); thin red solid contours are results from using the GRID set; blue dotted contours are results from using the MCMC-MARGE set, without pdf sampling.

fitter. We will leave this for future work. We also note that the significantly smaller marginalized errors (compared to likelihood errors) from the simulated data sets could be due to the simulated data sets not being sufficiently realistic. We will investigate this further in future work.

As SN Ia data increases in both quantity and quality, our method will be useful in the quest to illuminate the nature of dark energy using cosmological data.

ACKNOWLEDGEMENTS

We are grateful to Rick Kessler and Alex Conley for very helpful discussions. The computing for this project was performed at the OU Supercomputing Center for Education & Research (OSCER) at the University of Oklahoma (OU).

REFERENCES

Abell P. A. et al., 2009, LSST Science Book, Version 2.0, preprint ([arXiv:0912.0201](https://arxiv.org/abs/0912.0201))
 Bernstein J. P. et al., 2012, *ApJ*, 753, 152
 Betoule M. et al., 2014, *A&A*, 568, A22
 Branch D., 1981, *ApJ*, 248, 1076
 Brooks S. P., Gelman A., 1998, *J. Comput. Graph. Stat.*, 7, 434
 Caldwell R. R., Kamionkowski M., 2009, *Annu. Rev. Nucl. Part. Sci.*, 59, 397
 Conley A. et al., 2011, *ApJS*, 192, 1
 Contreras C. et al., 2010, *AJ*, 139, 519
 Frieman J., Turner M., Huterer D., 2008, *ARA&A*, 46, 385
 Guy J. et al., 2007, *A&A*, 466, 11

Guy J. et al., 2010, *A&A*, 523, A7
 Hamuy M. et al., 1996, *AJ*, 112, 2408
 Hicken M. et al., 2009, *ApJ*, 700, 331
 Jha S. et al., 2006, *AJ*, 131, 527
 Kessler R. et al., 2009, *PASP*, 121, 1028
 Laureijs R. et al., 2011, Euclid Definition Study Report, preprint ([arXiv:1110.3193](https://arxiv.org/abs/1110.3193))
 Lewis A., Bridle S., 2002, *Phys. Rev. D*, 66, 103511
 Li M., Li X.-D., Wang S., Wang Y., 2011, *Commun. Theor. Phys.*, 56, 525
 March M. C., Trotta R., Berkes P., Starkman G. D., Vaudrevange P. M., 2011, *MNRAS*, 418, 2308
 Mosher J. et al., 2014, *ApJ*, 793, 16
 Perlmutter S. et al., 1999, *ApJ*, 517, 565
 Phillips M. M., 1993, *ApJ*, 413, L105
 Phillips M. M., Lira P., Suntzeff N. B., Schommer R. A., Hamuy M., Maza J., 1999, *AJ*, 118, 1766
 Pskovskii Y. P., 1977, *Soviet Astron.*, 21, 675
 Ratra B., Vogeley M. S., 2008, *PASP*, 120, 235
 Riess A. G. et al., 1998, *AJ*, 116, 1009
 Riess A. G. et al., 1999, *AJ*, 117, 707
 Riess A. G., 2007, *ApJ*, 659, 98
 Sako M. et al., 2014, ([arXiv:1401.3317](https://arxiv.org/abs/1401.3317))
 Spergel D. et al., 2015, Wide-Field Infrared Survey Telescope—Astrophysics Focused Telescope Assets WFIRST-AFTA 2015 Report, preprint ([arXiv:1503.03757](https://arxiv.org/abs/1503.03757))
 Uzan J.-P., 2010, *Gen. Relativ. Gravit.*, 42, 2219
 Wang Y., 2010, *Dark Energy*, Wiley-VCH, Verlag GmbH & Co., Weinheim
 Weinberg D. H., Mortonson M. J., Eisenstein D. J., Hirata C., Riess A. G., Rozo E., 2013, *Phys. Rep.*, 530, 87

This paper has been typeset from a $\text{\TeX}/\text{\LaTeX}$ file prepared by the author.